Journal of Microwaves, Optoelectronics and Electromagnetic Applications, Vol. 21, No. 2, June 2022
DOI: http://dx.doi.org/10.1590/2179-10742022v21i2256950

Variations of Compact Rectangular Microstrip Antennas Using Defected Ground Plane Structure

Poonam A. Kadam[1], Amit A. Deshmukh[2]
[1]*Research Scholar, Electronics and Telecommunication Department, D J Sanghvi College of Engineering, India, poonam.kadam@djsce.ac.in*
[2]*Professor and Head, Electronics and Telecommunication Department, D J Sanghvi College of Engineering, India, amit.deshmukh@djsce.ac.in*

***Abstract* — The defects in the form of slots have been employed in microstrip antenna either on the patch or the ground plane to yield frequency reduction. However, the reported work does not provide any comparative study that highlight upon the frequency and cross-polar level reduction achieved using these various shape slot/defects. This paper provides a thorough comparative study for different compact variations of microstrip antennas obtained using various shape slots on the ground plane. Amongst all, the optimum results are obtained for the bowtie-shaped slot on the ground plane, which offers cross-polar level reduction by 30 dB with a frequency reduction of 21%. The study also reveals that the slot on the ground plane offers better results against the slot on the patch in terms of frequency and cross-polar reduction. This kind of comparative study is not available in the literature and thus this is the novelty in the present work. An empirical formulation for the resonant length at the fundamental mode frequency for different shapes of slot/defect is proposed. The frequency calculated using them closely matches with those obtained using the simulation.**

***Index Terms*—** Compact Microstrip antenna, Defected ground plane structure, Impedance bandwidth, Resonant length formulation, Cross polar radiation.

I. INTRODUCTION

Many wireless applications utilize microstrip antenna (MSA) owing to its features like lightweight, conformal, and ease of integration with RF microwave circuits. In these applications overall antenna size and polarization purity are the two major design considerations. Amongst several techniques to achieve the compactness, the slot cut technique is a well-known and promising method [1] – [3]. The slot have been introduced on the radiating patch to yield the patch size reduction or to achieve broadband or multiband response [4] – [11]. It is observed that the slot on the patch affect the input impedance matching and can degrade the pattern purity [1]. To avoid this, slots have been employed on the ground plane and such designs are referred to as defected ground plane structures (DGS) [34]. Using DGS designs, miniaturization in the patch size [12] – [16], enhancement in the impedance bandwidth (BW) [17] – [19], and multi-band response [20] – [24] have been realized. Many DGS configurations are reported in the past for reducing the antenna size. However, none of the reported

Brazilian Microwave and Optoelectronics Society-SBMO *received 4 Oct 2021; for review 5 Nov 2021; accepted 28 Mar 2022*
Brazilian Society of Electromagnetism-SBMag

ISSN 2179-1074

work on compact antenna designs have addressed upon reducing the cross-polar (XP) radiation together with the compactness. On the contrary, different DGS configurations by employing, slots on the ground plane are reported for reducing the XP radiation [25] – [30]. However, none of these designs provides a significant reduction in the patch resonance frequencies thereby yielding a compact structure. Further, the reported work does not discuss the basis for the selection of shape and location of the ground plane slot for yielding a compact design or to achieve lower XP radiation. Moreover, a comparative study that highlight upon the effects of the slot on the patch against that on the ground plane, is not available.

This paper presents a thorough comparative analysis for the MSAs backed by different slot shape ground plane against the slot on the patch. It provides a complete investigation on the impact of different slots profile on the resonance frequency and radiation pattern of the MSA, which is not discussed in this gravity in the literature. For every DGS compact design, through the parametric study, the optimum value of the slot dimensions is chosen for which an optimization in the values of frequency reduction and XP levels together is achieved. Further, the optimized DGS MSA is compared with the MSA having a similar slot dimension on the patch. Through this, the paper highlights the benefits of DGS antenna structures over antennas bearing slots on the patch, in terms of compactness and XP radiation. Amongst all the slot cut ground plane profiles, the bowtie-shape yields optimum results in terms of frequency and XP level reduction, gain, and bandwidth. The H-shape DGS yields the highest reduction in frequency. By studying the fundamental mode current distribution on the slot cut ground plane, resonant length formulation for the different ground plane profiles are proposed. The frequency calculated using them agrees closely with the simulated value. The proposed study is initially presented on FR4 substrate (ε_r = 4.3, tan δ = 0.02, h = 1.6 mm). Similar study has been carried out using RT Duroid substrate (ε_r = 2.33, tan δ = 0.001) that shows similar results. The CST software is used to analyze the response in various compact MSAs discussed here [32]. Thus, the present paper provides an in-depth study for the compact designs obtained using slots on the ground plane against that on the patch. It shows that DGS designs offer better results in terms of frequency and XP level reduction against the slot on the patch. This kind of detailed study is not available in the literature and thus this is the technical novelty in the proposed work.

II. COMPACT ANTENNA DESIGNS USING C AND H-SHAPED GROUND PLANE PROFILE

In different DGS designs in this paper, rectangular MSA (RMSA) of patch length L_p = 60 mm, patch width W_p = 60 mm, backed by ground plane of length L_g = 80 mm, and width W_g = 80 mm is selected, which is eventually modified by cutting slot on the ground plane. The RMSA without the ground plane slot resonates at the fundamental TM_{10} mode frequency of 1200 MHz on FR4 substrate. For the coaxial feed position at x_p = 18 mm, a detailed parametric study is carried out in each design to study the effects of slot dimension variation on the frequency and XP radiation level. In all the ground plane profiles discussed below, when the slot placed on the ground plane is orthogonal to the

Brazilian Microwave and Optoelectronics Society-SBMO *received 4 Oct 2021; for review 5 Nov 2021; accepted 28 Mar 2022*
Brazilian Society of Electromagnetism-SBMag *ISSN 2179-1074*

current directions at the fundamental mode, it results in current length perturbation on the ground. These modifications in current length are linked through the fringing fields present between the patch and ground to the modal currents on the patch that increases resonant length on the patch, which reduces the resonance frequency. The design of RMSA backed by a C-shape ground plane is shown in Fig. 1(a, b). The slot width *ls* and length w_s is cut on the ground plane below the non-radiating edge of RMSA.

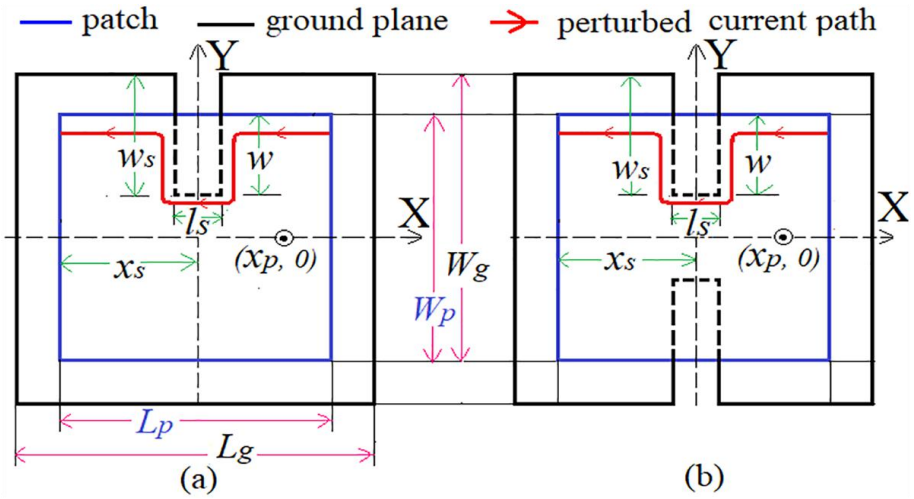

Fig. 1. Defected ground RMSA with (a) C-shape and (b) H-shape ground plane

The slot on the ground plane is placed at x_s = 30 mm, thus present exactly below the center of RMSA length that provides maximum frequency reduction at TM_{10} mode. The slot width w_s is cut with respect to the ground plane edge and thus w is the portion of the slot width that lies below the patch. For slot length l_s = 5 mm, w_s is increased in steps to study the effects on the frequency and XP level reduction. Various characteristics of the MSA are analyzed for varying slot widths and are listed in Table I. The slot width perturbs the current distribution on the ground and patch that results in TM_{10} mode frequency reduction. With an increase in w from 0 to 36 mm, TM_{10} mode frequency reduces by 44%. The higher-order TM_{02} mode frequency remains constant since the ground plane slot is located parallel to the surface currents at TM_{02} mode. Thus, with an increase in w, the separation between TM_{10} and TM_{02} mode frequencies increases that reduces the XP level at TM_{10} mode. In the parametric study, an optimum value of the slot width w is selected to be 24 mm, where the maximum possible reduction in the frequency and XP level together is achieved. Beyond this value, the XP level increases due to an increase in bidirectional current variation over the patch due to the C-shape slot on the ground plane. Thus frequency reduction for w = 24 mm is 29% and with the XP radiation level of -55 dB in the broadside direction. As seen from Table I, the input impedance for w = 24 mm, is 45 Ω. For realizing an optimum BW, the feed point is shifted towards the radiating edge. Optimum response in terms of the BW is realized for x_p = 23 mm. This yields simulated BW of 22 MHz (2.58%), without any changes in the other antenna parameters. The measured BW is 25 MHz (2.64%).

TABLE I. VARIOUS ANTENNA PARAMETERS FOR MSA BACKED BY C-SHAPE GROUND PLANE, x_p = 18 mm

received 4 Oct 2021; for review 5 Nov 2021; accepted 28 Mar 2022

ISSN 2179-1074

w_s (mm)	w (mm)	f_r, %Δf	Z_{in}(ohm)	BW, % BW (MHz, %)	Gain (dBi)	XP (dB)
0	0	1200, 0	60	28, 2.33	0.22	-20
14	4	1170, 2.5	48	32, 2.73	0.58	-31
18	8	1130, 5.8	40	30, 2.65	1.24	-32.5
22	12	1070, 10.8	36	25, .33	0.79	-39
26	16	990, 17.5	34	23, 2.32	0.14	-40
30	20	920, 23.3	39	21, 2.28	-0.69	-50
34	**24**	**850, 29**	45	**20, 2.35**	**-1.65**	**-55**
38	28	787, 34	58	18, 2.28	-2.74	-46
40	30	755, 37	64	17, 2.25	-3.4	-40
42	32	720, 40	65	14, 1.94	-4.1	-39
46	36	670, 44.16	81	10, 1.49	-5.4	-39.8

In each of the geometry discussed in this paper, the effective current path length is identified by considering the average current perturbation scenario due to the inclusion of the slot. To formulate the resonant length, surface current distribution at TM_{10} mode for RMSA backed by C-shape ground are studied on FR4 substrate. The current distribution for slot width of 20 and 30 mm are shown in Fig. 2(a, b). The current distribution with slot incorporated in the offset position, i.e. for $x_s = L_p/4$, is also shown in Fig. 2(c, d).

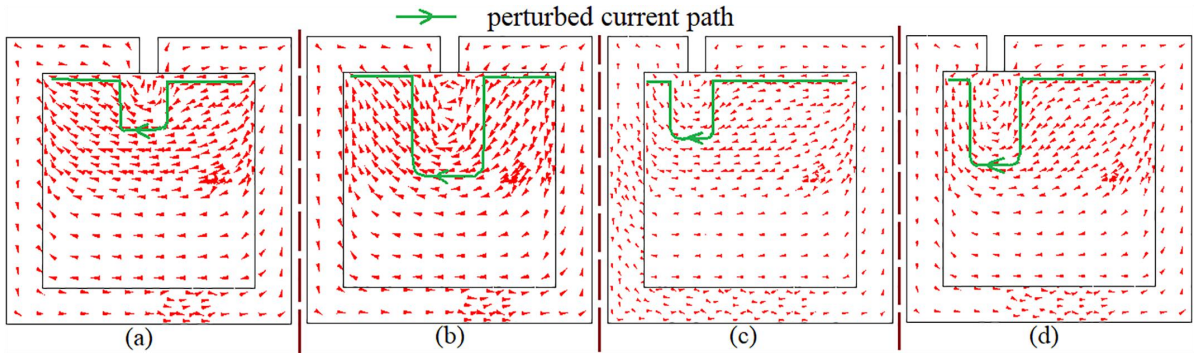

Fig. 2. Surface current distribution for RMSA backed by C-shape ground using FR4 substrate (a) $w_s = 20$, $x_s = 30$, (b) $w_s = 30$, $x_s = 30$, (c) $w_s = 20$, $x_s = 15$, (d) $w_s = 30$, $x_s = 15$

The current vectors in both cases are seen to be circulating around the slot. It is visible that the current path corresponding to the slot width of 30 mm is longer as compared to the 20 mm. The effective resonant length of the patch is computed by adding the incremental length of the current path due to the slots on the ground plane. This incremental length is a function of slot width w that is present below the patch and its location x_s from the RMSA edge, on the ground plane. At the fundamental mode of operation, half-wavelength variation is present along the patch length, which means the currents have a maximum value at the center of the patch and it decreases along the patch length. Towards the edges of the patch length, the minimum amplitude of the current is present. Also, the perturbation in the current path length is higher when the slot is placed nearer to the maximum current location and lower when it is placed nearer to the minimum current location [1]. Thus the

ISSN 2179-1074

current perturbation will be lesser at the offset position [1]. To accommodate for this positional relationship, the sinusoidal term is included in the resonant length equation as mentioned in (1). The perturbation in the surface current length is small for smaller slot width, while for larger slot width, it is larger. This variation is accounted for by the term A as mentioned in (1). The A is the constant and it maps the contribution of the slot dimension while doing the resonant length formulation. The value of A is selected to be 1.2, which is based on the variations observed in the fundamental mode frequency against the slot width. The effective resonant length (L_e) as given in (1) is the sum of patch length and the slot-induced incremental length. The resonant frequency is effectively influenced by the ground slot when the cut is made under the patch area. Hence the slot width w under the patch area is considered as given in (2). For the C-shape ground plane, since the current follows the slot contour, the increase in the length is by a factor $2w$, which is proportional to the ratio of w/W_p. The last term in (1) accounts for the fringing field extension present towards the radiating edges of the RMSA. The effective dielectric constant 'ε_{re}' in (1) is computed using the transmission line equation as given in [31]. Using (1) for L_e and the resonance frequency equation of RMSA, the frequency of RMSA backed by C-shape ground is calculated. The resonant frequencies as calculated using the above procedure for the center and offset slot positions matches closely with the simulated frequency as shown in Fig. 3, with % error less than 5%. Similar results are observed for MSA designed using RT-Duriod substrate.

$$L_e = L_p + 2\times A\times w\times \left(w/W_p\right) sin\left(\pi x_s/L_p\right) + 2h/\sqrt{\varepsilon_{re}} \tag{1}$$

$$w = w_s - \left(W_g - W_p\right)/2 \tag{2}$$

$$\%Error = \left(f_{cal} - f_{sim}\right)/f_{sim} \times 100\% \tag{3}$$

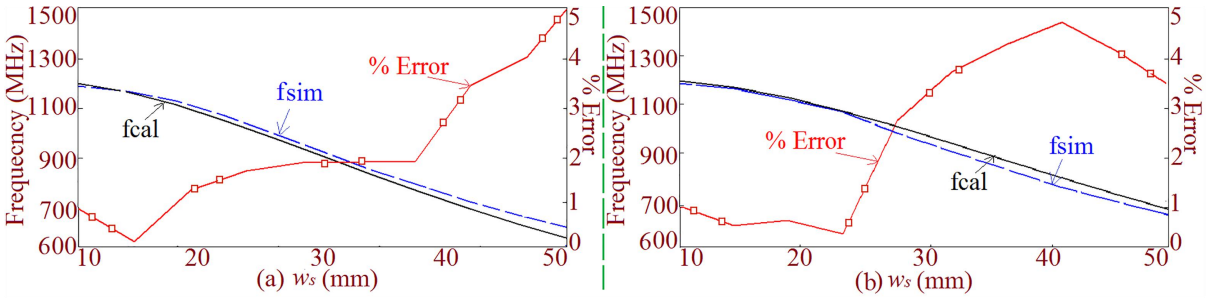

Fig. 3. Frequency and % error plots for (a) center slot (b) offset slot positions for RMSA backed by C-shape ground plane on FR4 substrate.

The design of RMSA backed by an H-shape ground plane is shown in Fig. 1(b). Against the C-shape, the H-shape ground plane is the symmetrical structure. The variations in various antenna parameters against the increase in the slot width w are illustrated in Table II. An optimum value of w is 24 mm, as

ISSN 2179-1074

with the further increase in the same, XP level increases. In the optimum case, resonance frequency reduces from 1200 to 659 MHz thereby providing 45% reduction and shows XP level of -50 dB in the broadside direction. For x_p = 18 mm, the input impedance (Z_{in}) is higher. The BW optimization is obtained for x_p = 15 mm, which gives simulated and measured impedance BW of 13 MHz (1.9%) and 15 MHz (2.2%), respectively as shown in Fig. 4(d). For this case, the XP level was observed to be -52 dB. The pattern response of this design was experimentally verified and radiation pattern and fabricated antenna for w = 24 mm are shown in Fig. 4(a – c). In the simulation, against the conventional ground plane, the XP level reduces from -20 dB to -52 dB. In the measurement, against the conventional ground plane, reduction in the XP level is from -12 to -38 dB. The difference in the XP level values is attributed to the measurement being carried out inside the Antenna laboratory against the anechoic chamber. The XP measurement is very sensitive to the reflections coming from the surrounding objects. Hence to remove the variations present in the lab environment against the ideal one (anechoic chamber), the measurement was carried out for the conventional ground plane also in the lab environment and against them the reduction in cross polar level using the modified ground plane was noted. As observed, in the simulation (ideal) and measurement, an equivalent amount of cross polar level reduction is observed, thereby verifying the proposed configuration.

TABLE II. RMSA BACKED BY H-SHAPE GROUND PLANE, x_p = 18 mm

w_s (mm)	w (mm)	f_r, %Δf (MHz,	Z_{in} (ohm)	BW, % BW (MHz, %)	Gain (dBi)	XP (dB)
0	0	1200, 0	60	28, 2.33	0.22	-20
14	4	1149, 4.25	36	34, 2.95	1.32	-40
18	8	1072, 10.6	31	25, 2.33	1.26	-53.8
20	10	1028, 14.3	30	21, 2.04	0.93	-42
24	14	933, 22.25	34	22, 2.3	-0.25	-45.2
26	16	888, 26	39	22, 2.47	-1.2	-46
30	20	780, 35	55	19, 2.43	-1.5	-47
34	**24**	**659, 45**	**81**	**12, 1.82**	**-1.52**	**-50**

The surface current distribution of H-shape DGS MSA for two slot lengths i.e. w_s = 20 and 30 mm is depicted in Fig. 4(e, f), respectively. Since the current follows the slot contour, an increase in the current path length is two times the slot width ($2w$) multiplied by the ratio of slot width by half of the patch width. The resulting equation is given in (4). Here the value of A is 1.4. The value of 'A' is calculated based upon the variation in the frequency against the slot width in the respective design. The resonant frequency for different slot widths is computed by applying the proposed formula.

$$L_e = L_p + 4 \times A \times w \times \left(w / W_p \right) sin\left(\pi x_s / L_p \right) + 2h / \sqrt{\varepsilon_{re}} \tag{4}$$

ISSN 2179-1074

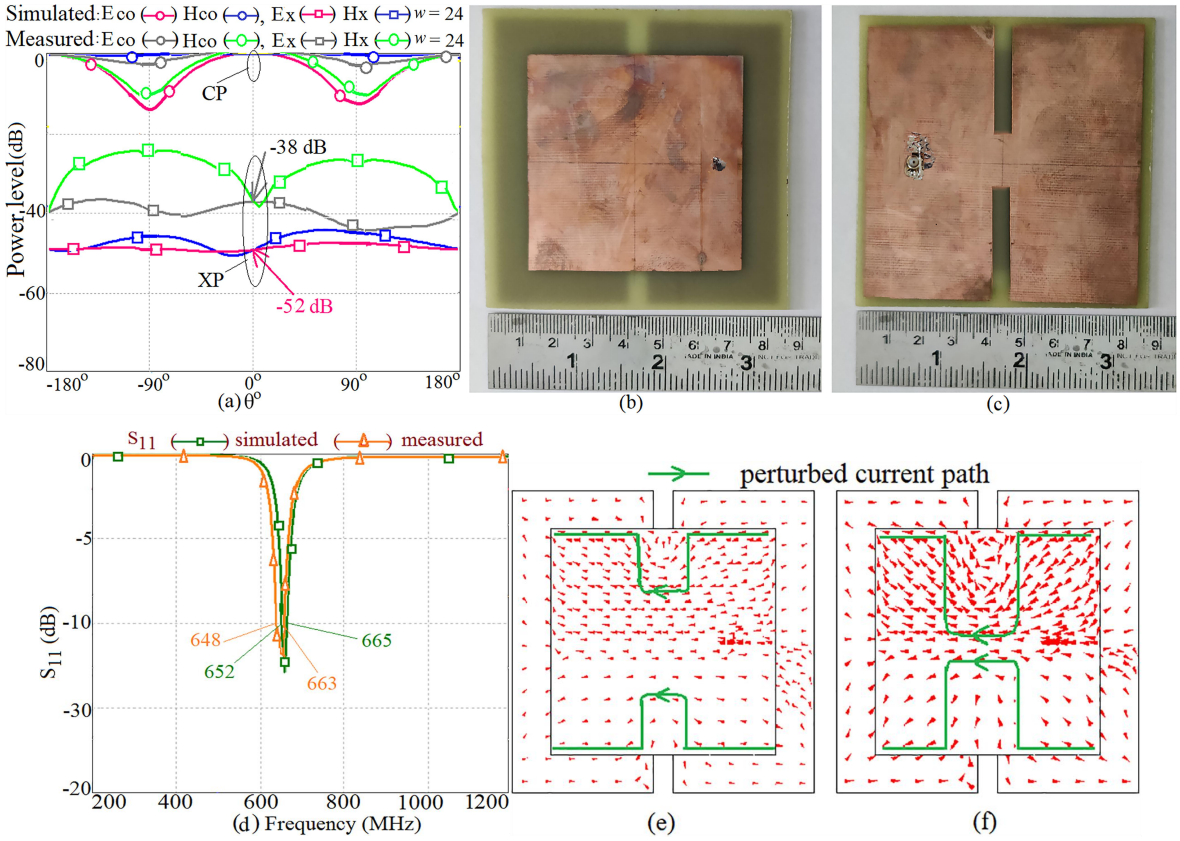

Fig. 4. (a) Radiation pattern (b, c) fabricated prototype, and its (d) return loss plot (S_{11} plot) for optimum design of MSA backed by H-shape ground plane, for w = 24, current distribution for slot length (e) w_s = 20 (f) w_s = 30

III. COMPACT ANTENNA DESIGNS USING CENTER SLOT AND RING-SHAPED GROUND PLANE PROFILE

The RMSA backed by a narrow rectangular slot ($l_s < w$) cut ground plane is shown in Fig. 5(a). Through the parametric study, an optimum slot width w is found to be 26 mm for which a XP level of -49 dB is observed in the broadside direction, which is also accompanied by 15% reduction in the frequency. The result for the same is provided in Table III. For w = 26 mm, the BW optimization is achieved for x_p = 9 mm, yielding impedance BW of 21 MHz (2.05%) and XP level of -43 dB. Here, measured BW and XP levels in the broadside direction are 24 MHz (2.3%) and -32 dB, respectively.

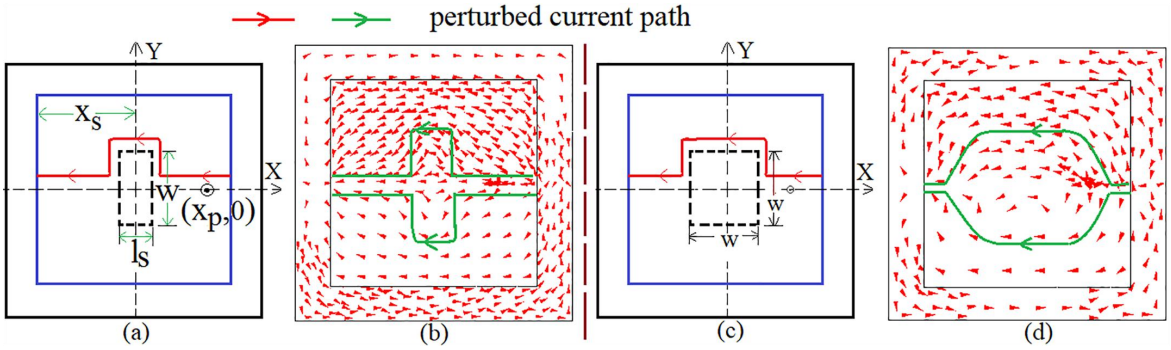

Fig. 5. (a) RMSA backed by a rectangular slot cut ground plane, its (b) surface current plot for w = 20 mm, (c) RMSA backed by ring shape ground, its (d) current plot for w = 20 mm

received 4 Oct 2021; for review 5 Nov 2021; accepted 28 Mar 2022

ISSN 2179-1074

The current distribution for rectangular slot width of 30 mm is shown in Fig. 5(b). For the narrow rectangular slot cut ground plane, the surface currents follow the slot edges. As the structure is symmetrical, an increase in the current path length is two times half of the patch width i.e. 2(*w*/2). The modified resonant length expression for this design is given in (5). For this design, the value of '*A*' is 1.1. Against the slot width variation, calculated frequencies obtained using this equation agrees closely with the simulated frequencies with an % error of less than 5 %.

$$L_e = L_p + A \times w \times \left(w / W_p \right) sin\left(\pi x_s / L_p \right) + 2h / \sqrt{\varepsilon_{re}} \tag{5}$$

TABLE III. RMSA BACKED NARROW RECTANGULAR SLOT CUT GROUND PLANE, x_p = 18 mm

w (mm)	f_r, %Δf (MHz, %)	Z_{in} (ohm)	BW, % BW (MHz, %)	Gain (dBi)	XP (dB)
0	1200, 0	60	28, 2.33	-0.01	-20
14	1140, 5	73	24, 2.1	-0.7	-37
18	1102, 8.2	78	22, 1.99	-1.47	-41
22	1046, 12.8	88	17, 1.62	-1.8	-34
26	**1020, 15**	**91**	**14, 1.37**	**-1.9**	**-49**

Based on the simple C-shape, H-shape and the rectangular slot cut ground plane MSAs, other variations of DGS MSA are developed. By realizing equal dimension for the slot width and length, the ground plane is transformed into a ring shape design. In the ring shape ground plane, a square slot is cut in the center as shown in Fig. 5(c). The study to analyse the effects of ring slot dimensions on the antenna parameters is carried out, as tabulated in Table IV. An optimum value of the ring slot dimension is found to be 15 x 15 mm, at which the XP level in the broadside direction is minimum. The XP level increases when the slot dimensions are increased further. For the above ring slot dimension, frequency reduces from 1200 to 1095 MHz, thereby providing 8.75% frequency reduction. Here the impedance BW observed for Z_{in} = 82 Ω, is 23 MHz (2.1%). The impedance BW observed in the measurement is 28 MHz (2.5%). The shift in the feed point location to realize 60 - 65 Ω impedance matching, shows marginal changes in the BW. As the surface current follows the path that is surrounding the slot as shown in Fig. 5(d), an increase in the current path length is 2(*w*/2), multiplied by the ratio, slot width to the patch width, as given in (6). In this design 'A' equals 1.3. The frequencies computed using (6) match closely with the simulated frequencies for varying slot width with an % error of less than 5%. Thus as compared with the previous slot cut DGS designs, ring MSA does not provide better results in terms of frequency and XP level reduction. This is attributed to the shape of the ring geometry where the slot dimensions are increasing along both the axis.

$$L_e = L + A \times w \times \left(w / W_p \right) + 2h / \sqrt{\varepsilon_{re}} \tag{6}$$

ISSN 2179-1074

TABLE IV. RMSA BACKED RING SHAPE GROUND PLANE, x_p = 18 mm

w (mm)	f_r, %Δf (MHz, %)	Z_{in} (ohm)	BW, % BW (MHz, %)	Gain (dBi)	XP (dB)
0	1200, 0	60	28 2.33	0.18	-20
5x5	1190, 0.8	65.8	27, 2.3	-0.15	-19
10x1	1145, 4.8	72	25, 2.2	-0.6	-24
15x1	**1095, 8.75**	**82**	**23, 2.1**	**-0.5**	**-27**
20x2	1032, 14	100	07, 0.7	-0.5	-21

IV. COMPACT ANTENNA DESIGNS WITH MULTIPLE GROUND SLOTS

The variations of RMSA backed by multiple rectangular slots cut ground planes are presented in this section. Instead of single slot, multiple slots placed at equally spaced positions can have more controlled reduction in the frequency, hence these variations are studied here [1]. The RMSA backed by two slot cut ground plane is shown in Fig. 6(a). In this design, slots are placed inside the ground plane area whereas in the second design as shown in Fig. 7(a), slots are placed on the ground plane edges. The results of the parametric study with slots inside the ground plane are illustrated in Table V. This configuration is similar to the center rectangular slot cut design, but with a offset slots, i.e. $x_s = L_p/4$. Since the study is presented at the fundamental TM_{10} mode, any position other than in the center ($x_s = L_p/2$), will yield a smaller frequency reduction. Thus to ensure the symmetry with reference to the patch radiating edges, slot position at $L_p/4$ is chosen here. An optimum value of the slot width *w* is found to be 16 mm, for which the input impedance matching is obtained.

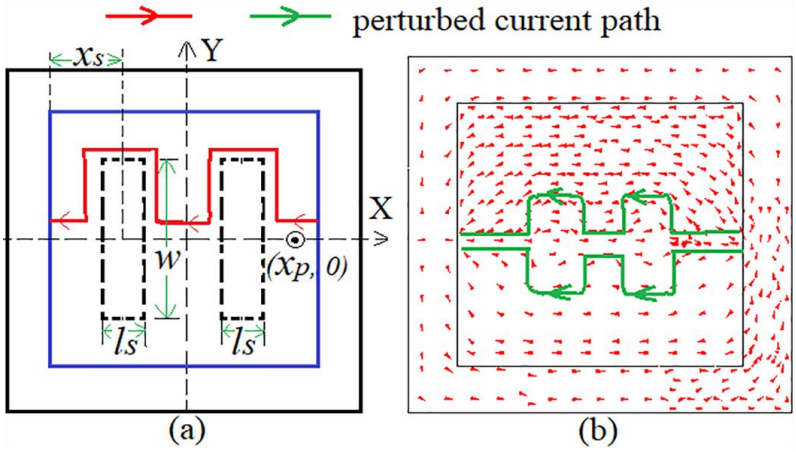

Fig. 6. (a) Structure of RMSA with two rectangular slots on the ground plane (b) surface current plots for the ground plane with slots at *w* = 20 mm

TABLE V. RMSA BACKED BY TWO RECTANGULAR SLOTS CUT GROUND PLANE, x_p = 18 mm

w (mm)	f_r, %Δf (MHz, %)	Z_{in} (ohm)	BW, % BW (MHz, %)	Gain (dBi)	XP (dB)
0	1200, 0	60	28, 2.33	0.18	-20
12	1140, 5	81	22, 1.93	-0.3	-27
16	**1100, 8.3**	**95**	**15, 1.36**	**-0.7**	**-31**

ISSN 2179-1074

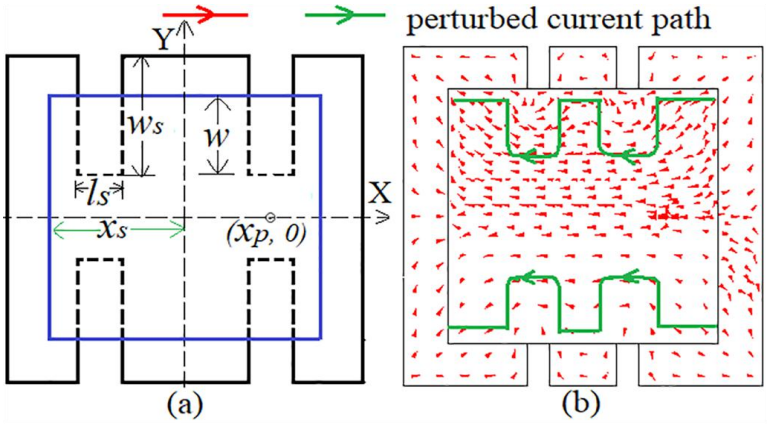

Fig. 7. (a) Structure of RMSA backed by H-shape cut ground plane (b) surface current plots for the ground plane with slots at w = 20 mm

For, w = 16 mm, reduction in the frequency is from 1200 to 1100 MHz, thus providing 8.3% reduction. With respect to the conventional ground plane, XP level reduction is by 11 dB. For x_p = 18 mm, Z_{in} is higher. Thus, an optimum BW is achieved for x_p = 15 mm. Here, the simulated BW is 19 MHz (1.72%) whereas the BW achieved using measurement is 23 MHz (2%). The surface current distribution for this slot cut ground plane is shown in Fig. 6(b). An increase in the current path length is twice that of the single rectangular slotted DGS RMSA as given in (5). The resulting expression with two slots is given in (7). The frequency calculated using (7) against varying slot width matches closely with those obtained using the simulation, with % error less than 5%.

$$L_e = L_p + 2 \times w \times \left(w / W_p \right) sin\left(\pi x_s / L_p \right) + 2h / \sqrt{\varepsilon_{re}} \tag{7}$$

The RMSA backed by dual H-shape cut ground plane as shown in Fig. 7(a) is obtained by cutting two open-ended rectangular slots on each of the horizontal edges of the ground plane. The parametric study on varying the slot width is carried out and results for the same are given in Table VI. Here an optimum value of the slot width w is found to be 16 mm, as the XP level in the broadside direction is 31 dB down as against the XP level obtained with the conventional ground plane. This slot width also offers 30% frequency reduction; i.e. from 1200 to 839 MHz. For w = 16 mm, an optimum BW is obtained for x_p = 25 mm. Here the simulated BW is 30 MHz (3.97%), whereas the measured BW is 34 MHz (4.05%), as shown in Fig 8(b). The simulated and measured radiation pattern plots for the MSA backed by dual H-shape ground plane for w = 16 mm are shown in Fig. 8(a). The radiation pattern is observed in the broadside direction with E and H planes aligned along $\phi = 0^0$ and 90^0, respectively. With reference to the conventional ground plane, in the simulation, the XP level has reduced from -20 to -53.2 dB, whereas in the measurement, the same has reduced from -12 to -40 dB. Thus in the two cases, a comparable amount of XP level reduction is observed. The fabricated antenna is shown in Fig. 8(c, d). The surface current distribution for dual H-shape ground plane design is shown in Fig. 7(b). Since this structure is an extension of H-shape ground MSA, the increase in the resonant length is

ISSN 2179-1074

twice that of the H-shape ground MSA. Using the parametric study, the value of A is selected to be 1.1. The resonant length equation for this design is given in (8). Further, frequencies calculated using (8) and the resonance frequency equation of RMSA [1], against increasing slot width matches closely with those obtained using the simulation, with % error less than 5%.

$$L_e = L + 8 \times A \times w \times \left(w / W_p \right) sin\left(\pi x_s / L_p \right) + 2h / \sqrt{\varepsilon_{re}} \tag{8}$$

TABLE VI. RMSA BACKED BY DUAL H-SHAPE GROUND PLANE, x_p = 18 mm

w_s (mm)	w (mm)	f_r, %Δf (MHz,	Z_{in}(ohm)	BW, % BW (MHz,	Gain (dBi)	XP (dB)
0	0	1200, 0	60	28, 2.33	0.18	-20
14	4	1127, 6.08	27.8	26, 2.3	1.62	-57
26	**16**	**839, 30**	**37**	**21, 2.5**	**1.1**	**-51**
30	20	730, 39	56	19, 2.6	-1.2	-45

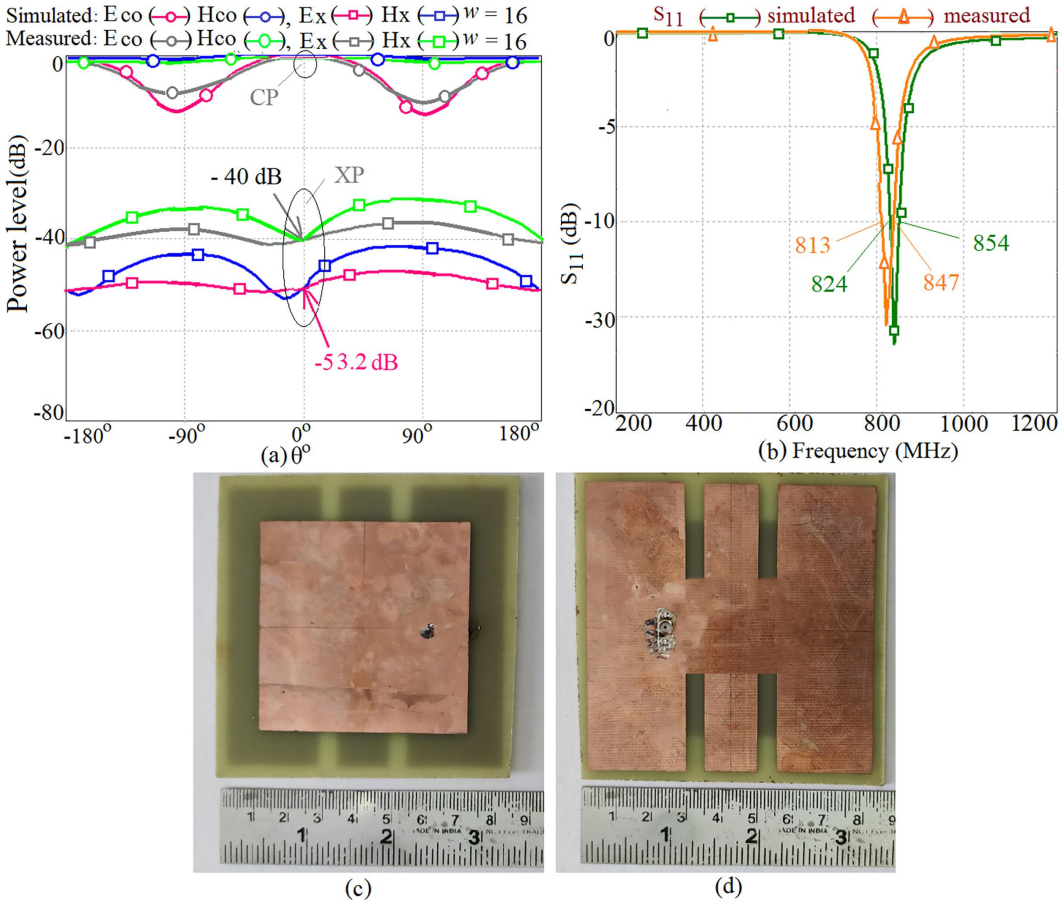

Fig. 8. (a) Radiation pattern and (b) S_{11} plot (c, d) fabricated prototype of optimum design of MSA backed by dual H-shape ground plane, for w = 16.

The design of RMSA backed by a W-shape ground plane is shown in Fig. 9(a). The W-shape structure is realized by cutting two slots on the top horizontal ground plane edge and a single rectangular slot on the bottom edge. The results for the parametric study on varying slot width is illustrated in Table VII. An optimum value of the slot width w is found to be 15 mm, where the 15% frequency reduction

ISSN 2179-1074

is obtained. For this width, the XP level in the broadside direction is 25 dB down as compared with the conventional ground plane design. The BW optimization is achieved by shifting the feed point location to x_p = 15 mm. For this, the simulated and measured impedance BW is 16 MHz (1.9%) and 18 MHz (2%), respectively. Due to three slots present on the two opposite edges, for the resonant length estimation, three current path lengths, L_1, L_2, and L_3 exist, as shown in Fig. 9(a – d). Depending upon the horizontal separation between the three slots, resonant length estimation changes in this design. Hence the resonant length formula is provided for the three cases based upon the separation between the two slots *d* on one edge. The current distribution plots for the three cases are shown in Fig. 9(b – d). Based on these current paths, various current path lengths are formulated in (9) – (12).

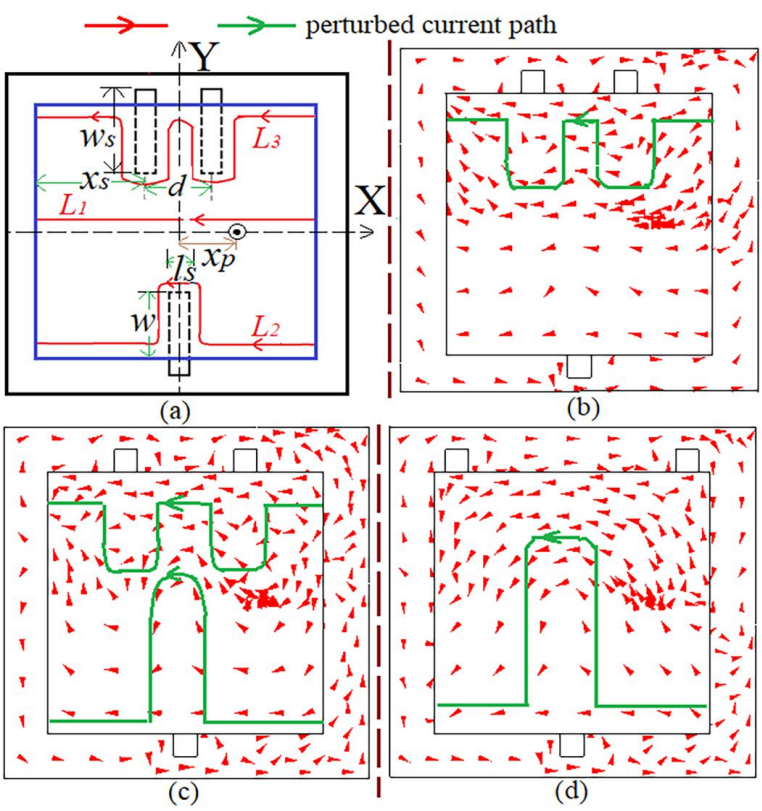

Fig. 9. (a) RMSA backed by W-shape ground plane and its current distribution for w_s = 30mm (b) small *d* (*d* = 5mm), (c) intermediate *d* (*d* = 15 mm), (d) large *d* (*d = 25 mm)*

TABLE VII. RMSA BACKED BY THREE RECTANGULAR SLOTS CUT GROUND PLANE WITH d = 15, x_p = 18 mm

w_s (mm)	w (mm)	f_r, %Δf (MHz,	Z_{in}(ohm)	BW, % BW (MHz,	Gain (dBi)	XP (dB)
0	0	1200, 0	60	28, 2.33	0.18	-20
10	5	1160, 3.3	58	27.4, 2.36	0.5	-33
15	10	1084, 9.6	56	25, 2.3	-0.08	-50
20	15	985, 18	71	22, 2.25	-1.12	-39
25	**20**	**873, 27.25**	**83**	**16.6, 1.9**	**-2**	**-55**

ISSN 2179-1074

$$L_1 = L_p \tag{9}$$

$$L_2 = L + 2w \tag{10}$$

$$L_3 = L + 4w \times \left(w / W_p \right) \times sin\left(2\pi x_s / L_p \right) \tag{11}$$

$$L_e = \left(L_1 + L_2 + L_3 / 3 \right) + 2h / \sqrt{\varepsilon_{re}} \tag{12}$$

The equation given in (9) corresponds to the current path in absence of the slots, i.e. for RMSA. The equation given in (10) corresponds to the resonant length formula due to the presence of only a single slot present at the bottom non-radiating edge. As the slot is present at the center of patch length, current perturbation is maximum here. Hence the equation given in (10) does not include the sinusoidal term for TM_{10} mode current variation. The equation given in (11) corresponds to the resonant length formula due to the presence of two slots that are below the other non-radiating edge of the RMSA. In W-shape MSA ground plane design, when the slots are small i.e. $w < 0.3W_p$, effective resonant length can be calculated by using an average of three current paths, i.e. an average of (9), (10) & (11) as mentioned in (12). For slot length larger than $0.3W_p$, the effective resonant length is a strong function of separation between slots. When slots are very close, these slots become dominant, and resonant surface currents follow the path along with these slots as shown in Fig. 9(b) and are deduced by adding fringing fields effect to (11). Whereas, when slots are far distant, the slot on the other side becomes dominant and the surface current path is shown in Fig. 9(d) and the current length expression is given in (10). For intermediate slot separation (Fig. 9(c)), an average of (10) & (11) gives the effective resonant length. Frequencies calculated using (12) for varied slot length and separation match closely with those obtained by using the simulation showing % error less than 5%.

V. COMPACT ANTENNA DESIGNS USING BOWTIE-SHAPED GROUND PLANE

The design of RMSA backed by a bowtie-shape ground plane is shown in Fig. 10(a). The results for the parametric study on varying slot depth w is illustrated in Table VIII. An optimum value of w is found to be 16 mm, as it offers a frequency reduction of > 20% with XP level reduction of more than 30 dB against the conventional ground plane design. For w = 16 mm and x_p = 28 mm, an optimum BW of 42 MHz (4.42%) with XP level of -56 dB and broadside gain of 1.01 dBi, is achieved. Here the measured BW is 47 MHz (4.95%). An improvement in the BW and gain in the bowtie-shaped ground plane design is attributed to the more detachment of fringing fields from the slotted ground plane area and thereby focussing them in the broadside direction due to the bowtie structure. By observing the surface current distribution as shown in Fig. 10(b), resonant length is formulated as given in (13). The values of 'y' and 'b' are computed by applying the triangle property given in (14)

Brazilian Microwave and Optoelectronics Society-SBMO *received 4 Oct 2021; for review 5 Nov 2021; accepted 28 Mar 2022*
Brazilian Society of Electromagnetism-SBMag *ISSN 2179-1074*

& (15). The frequency calculated using (13) for varied slot depth, matches closely with simulated results with an error of less than 5%.

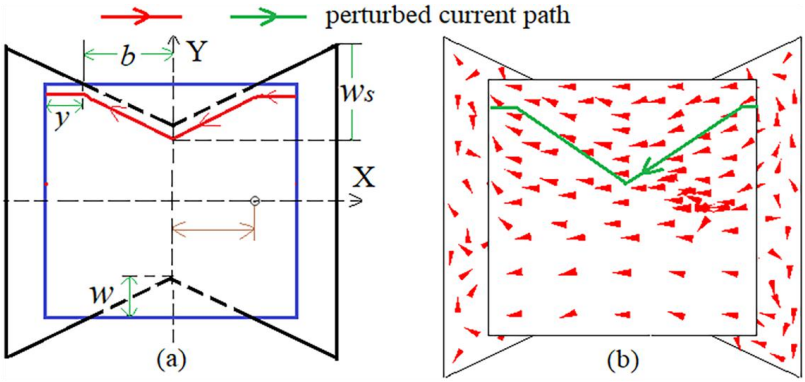

Fig. 10. (a) RMSA backed by bowtie-shaped ground plane and its, (b) surface current distribution for $w_s = 20$ mm

$$Le = 2y + 2\sqrt{(b)^2 + \left((w)^2\left(w/W_p\right)\right)} \tag{13}$$

$$y = \left(L_p/2\right) - b \tag{14}$$

$$b = \left(L_g w/2w_s\right) \tag{15}$$

TABLE VIII. RMSA BACKED BY BOWTIE-SHAPED GROUND PLANE, $x_p = 18$ mm

w_s (mm)	w (mm)	f_r, %Δf (MHz, %)	Z_{in} (ohm)	BW, % BW	Gain (dBi)	XP (dB)
0	0	1200, 0	60	28, 2.33	0.18	-20
14	4	1140, 5	32	48, 4.2	1.9	-57
18	8	1080, 10	28	47, 4.35	1.64	-51.7
22	12	1019, 15	29	44, 4.31	1.25	-51.5
24	14	990, 17.5	30	44, 4.44	1.01	-56
26	**16**	**949, 21**	**34**	**28, 2.95**	**0.6**	**-56.2**
30	20	878, 27	47	30, 3.41	0.65	-51

The antenna parameters obtained in the optimum configurations in each of the modified ground plane RMSAs are compared in Table IX. Using the conventional ground plane, in simulation, the XP level in the broadside direction is -20 dB. In all the proposed slot cut ground plane profiles, the XP level reduction supported with the resonance frequency reduction is achieved. Amongst them, optimum results are realized in the H-shape ground plane profile where the frequency reduction of 45% with a XP level reduction by more than 30 dB is achieved. In comparison to the H-shape, in bowtie-shaped ground plane design, improvement in the BW and gain is also observed. However, the frequency reduction is smaller here. Thus, specifically in terms of compactness supported with the XP level, the H-shape design offers optimum results. In all the DGS compact designs, the radiation pattern is in the broadside direction with E and H planes aligned along with $\Phi = 0^0$ and 90^0 respectively. The

received 4 Oct 2021; for review 5 Nov 2021; accepted 28 Mar 2022

ISSN 2179-1074

radiation pattern measurement of the proposed antennas is carried out in the laboratory deploying the setup shown in Fig. 11(a). For measuring the radiation pattern, a reference high gain wideband horn antenna is used. The spacing between the horn antenna and the antenna under test (proposed DGS MSA) is kept to be more than $2D^2/\lambda_o$ to satisfy the far-field condition. Here 'D' is the maximum aperture dimension of the horn antenna. The impedance measurement setup is shown in Fig. 11(b). As we know the XP level is very sensitive to the pattern measurement, hence we have ensured minimum reflection from the surrounding objects in the lab with respect to frequency of operation. Also, the required far-field distance was maintained. As the measurement is carried out other than the anechoic chamber deviation in the measured XP levels against the simulation is expected. To verify our concept for the proposed design the pattern measurement in the lab environment was carried out for modified as well as conventional ground plane (without slot) antenna. If for a certain design x dB of XP reduction in the broadside direction is observed in the simulation going from conventional to modified ground plane design, a similar amount of reduction (a value close to x dB) is noted in the measurement as well. And thus here by doing measurement for the conventional ground plane MSA also, we are removing the errors in the XP measurement against the ideal environment for the proposed configuration (simulation & anechoic chamber).

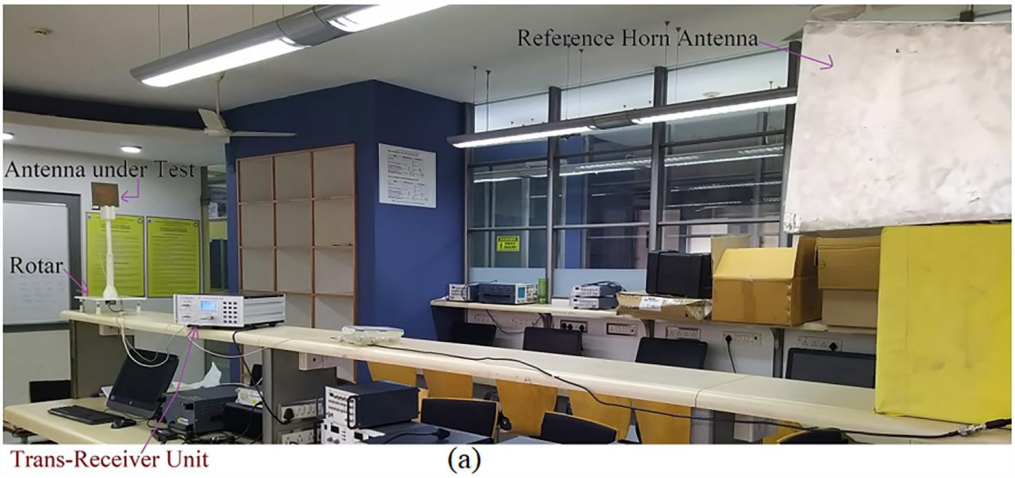

Fig. 11. (a) Radiation pattern and (b) impedance measurement set up

ISSN 2179-1074

TABLE IX. OPTIMUM SLOT CUT MSAS BACKED BY A DIFFERENT SLOT CUT GROUND PLANE

Ground plane profile	*w* (mm)	f_r, $\%\Delta f$ (MHz,	BW, % BW (MHz,	Gain (dBi)	XP (dB)
C-shape ground plane	24	850, 29.2	22, 2.58	-1.65	-55
H- shape ground plane	**24**	**659, 45**	**13, 1.9**	**-1.52**	**-52**
Rectangular cut on ground	26	1020, 15	21, 2.05	-1.9	-43
Ring shape ground plane	15	1095, 8.75	23, 2.1	-0.6	-24
Dual rectangular slot	16	1100, 8.3	19, 1.72	-0.7	-31
Dual H- shape ground plane	16	839, 30	21, 2.5	1.1	-53
Three rectangular slots	20	875, 27	18, 2	-2.2	-51
Bowtie-Shaped ground plane	**16**	**949, 21**	**42, 4.42**	**1.0**	**-56**

Further, an optimum configuration in each of the DGS RMSAs is compared with a similar RMSA bearing slot on the patch for a fixed feed point location, x_p = 18 mm. The comparison for them is presented in Table X. In each DGS design, against the slot on the patch, a reduction in the XP radiation level in the broadside direction is noted. Further, C-shape, H-shape, dual H-shape and bowtie-shape configurations on the ground plane offer higher frequency reduction as against that on the patch. Thus, slot on the ground plane offers clear advantages against that on the patch. This kind of detailed study for various compact DGS designs against compact MSAs using the slot on patch has not been reported in the literature. Thus, a thorough comparative study for various DGS designs with their comparison against compact MSAs bearing a slot on the patch is the new contribution in the present work.

Further, optimum configurations of H-shape and bowtie-shaped ground plane profiles are compared against some of the reported designs using non-DGS and DGS, offering compactness, wideband response, and low XP radiation levels. The comparison for them is presented in Table XI. In the wideband non-DGS and DGS designs reported in [11, 17, 18, 19, 26], BW of more than 50% is achieved. However, these designs do not offer a significant reduction in the fundamental mode frequency as well as the reduction in the XP levels. The designs presented in [12, 16] do offer reduction in the fundamental mode frequency but the reduction in the XP levels is absent. In the proposed DGS configurations, RMSA backed by H-shape DGS offers a substantial reduction in the frequency as well as XP level, whereas bowtie DGS design offers improvement in BW and gain with moderate values of the frequency reduction and a good amount of reduction in the XP levels. In addition, these two designs require smaller substrate thickness against the reported variations. Although similar designs of regular shape MSA backed by bowtie-shaped ground plane are reported in [33]. However, those designs only discuss the use of bowtie-shaped DGS and thus does not provide a detailed study of using other ground plane profiles. Thus to summarize, the present paper provides a detailed study that compares various compact configurations obtained by employing different DGS shapes. The comparison is highlighted for frequency reduction obtained along with the XP reduction achieved. Here, reported papers either discuss the compact designs using DGS or XP level reductions using DGS. They do not describe in detail, effects on the corresponding other parameters.

Brazilian Microwave and Optoelectronics Society-SBMO *received 4 Oct 2021; for review 5 Nov 2021; accepted 28 Mar 2022*
Brazilian Society of Electromagnetism-SBMag *ISSN 2179-1074*

TABLE X. COMPARISON AMONG DIFFERENT SLOT CUT MSAS AT x_p = 18 mm

MSA variations	w (mm)	Slot on the patch		Slot on the ground plane	
		f_r, %Δf (MHz,	XP (dB)	f_r, %Δf	XP (dB)
C-Shape	24	875, 27	-31.2	850, 29.2	-55
H-Shape	**24**	**695, 42**	**-34**	**659, 45**	**-50**
Rectangular slot cut	26	1018, 15.1	-33.8	1020, 15	-43
Ring Shape	15	1095, 8.75	-15.6	1095, 8.75	-24
Dual Rectangular slot cut	16	1102, 8.1	-22	1100, 8.3	-31
Dual H-shape	16	884, 26.3	-30.7	839, 30	-51
Three rect. slot cut	20	796, 33	-32	873, 27	-55
Bowtie-shape	**16**	**1014, 15**	**-31.6**	**949, 21**	**-56**

TABLE XI. COMPARISON OF H-SHAPE AND BOWTIE-SHAPE DGS DESIGNS AGAINST REPORTED MSAS

MSA shown in	f_c	% Δ	BW, % (MHz, %)	Gain (dBi)	XP (dB)	h/λ_g	A/λ_g
Fig. 1(b)	**659**	**45%**	**13, 1.9**	**-1.52**	**-52**	**0.007**	**1.64**
Fig. 9(a)	**949**	**21%**	**42, 4.42**	**1.0**	**-56**	**0.009**	**2.19**
[11]	3000	-	2040, 68	9.6	< -34	0.02	2.3
[12]	3000	50%	-	2.1	-	0.03	0.323
[16]	1800	77%	81, 4.5	0.43	-	0.02	0.5
[17] Circular ground	7900	-	6850, 86.79	4.1	-	0.06	0.163
[17] Square ground	7900	-	5999, 75.94	2.39	-	0.06	0.163
[18]	6950	3.4%	7700, 110	5.1	-20	0.077	0.25
[19]	1220	-	7100, 58	9.2	-30	0.097	0.47
[25] Square	1010	-	710, 7	6.2	-40	0.08	0.36
[25] Circular	1010	-	660	6.1	-40	0.08	0.4
[26]	1000	0.5%	1000, 10	-	-43	0.08	0.29
[27]	1068	0.3%	-	5.1	-41	0.08	0.279
[28]	1000	-	800	-	-46	0.08	0.4

Further, a comparison between the slot on the patch against the slot on the ground plane in yielding compactness is discussed in the present work. All the DGS designs offer a reduction in frequency with XP level reduction. The XP reduction is not achieved with slots on the patch. Thus, a detailed comparative study to present a difference between using the slot on a patch against that on the ground plane (DGS) in achieving compactness in addition to XP level reduction is the new technical contribution in the present work. Although various designs using DGS are reported in the literature, but this kind of insight is absent. The experimental verification for the obtained results is carried out inside the Antenna Lab. In all the designs, a similar reduction in the frequency and XP levels to that obtained in the simulation is observed, thus verifying the obtained results and the proposed concept. Further for the same patch and ground plane dimensions, similar study using different DGS designs and their comparative study with slot on the patch has been carried out using low loss RT Duriod substrate. The study using other substrate parameter and thus the frequency, shows similar results in terms % frequency and XP reduction achieved in DGS designs to that obtained with slot employed on the patch.

ISSN 2179-1074

VI. CONCLUSIONS

This paper presents a thorough comparative study of various compact variations of MSA obtained by etching various shape slots on the ground plane (DGS) against that on the radiating patch. Amongst all the variations, H-shape DGS yields maximum compactness, broadside XP levels less than -50 dB, and over less than 30 dB XP radiation over ± 180^0 angular range. The best optimum results in terms of all the antenna parameters are obtained in a bowtie-shaped configuration. Here broadside XP level as low as -56 dB with less than 30 dB XP radiation over ±180^0 angular range, 21% size reduction with a gain of 1 dBi, is achieved on a thinner and lossy substrate. The DGS MSAs compared with the slot on the patch offer better polarization purity for all the configurations discussed in the paper with more reduction in the frequency (compactness). This highlights the benefit of cutting slots on the ground plane in place of the patch. The empirical formulations to estimate the resonant length of MSAs backed with different ground plane profiles are proposed in this paper. Frequencies calculated using them closely agree with those obtained using simulation. Thus, the proposed work provides a detailed comparative analysis for DGS MSAs against slots on the patch and thus highlights the benefits of using compact structures using DGS profiles.

REFERENCES

[1] G. Kumar and K. P. Ray, *Broadband Microstrip Antenna*, USA: Artech House, 2003.
[2] A. A. Deshmukh, and Kumar, G., "Formulation of Resonant frequency for Compact Rectangular Microstrip Antennas", *Microwave and Optical Technology Letters*, vol. 49, (2), pp. 498-501, 2007.
[3] S. Dey and R. Mittra, "Compact Microstrip Patch Antenna", *Microwave and Optical Technology Letter*, vol. 13, pp. 12-14, 1996.
[4] K. Wong, *Compact and Broadband Microstrip Antenna*, USA: Wiley & Sons, 2002.
[5] K. L. Wong and K. P. Yang, "Compact dual Frequency microstrip antenna with a pair of bent slot", *Electronics Letters*, vol. 34, 225-226, 1998.
[6] J. Lu and K. Wong, "Slot loaded meandered rectangular microstrip antenna with compact dual-frequency operation", *Electronics Letter*s, vol. 34, pp. 1048-1050, 1998.
[7] A. A. Deshmukh and K. P. Ray, "Analysis of L-shape slot cut broadband rectangular microstrip antenna", *International Journal of Electronics*, vol. 59, pp. 1108-1117, 2013.
[8] K. F. Lee, K. M. Luk and K. F. Tong, "Experimental and simulation studies of the coaxially fed U-slot rectangular patch antenna", *IEE Proceedings - Microwaves, Antennas and Propagation*, vol. 144, pp. 354-358, 1997.
[9] K. F. Lee, K. M. Luk, K. M. Mak and S. L. Yang, "On the use of U-slots in the design of dual and triple-band patch antennas", *IEEE Antennas and Propagation Magazine*, vol. 53, pp. 60-74, 2011.
[10] K. F. Lee, S. L. Yang and A. A. Kishk, "Dual and multiband U-slot patch antennas", *IEEE Antennas and Wireless Propagation Letters*, vol. 7, pp. 645-647, 2008.
[11] S. Radavaram and M. Pour, "Wideband Radiation Reconfigurable Microstrip Patch Antenna Loaded with Two Inverted U-Slots", *IEEE Transactions On Antennas and Propagation*, vol. 67, pp. 1501-1508, 2019.
[12] H. Elftouh, N. Touhami, M. Aghoutane, S. Amrani, A. Tazon and M. Boussouis, "Miniaturized microstrip patch antenna with defected ground structure", *Progress in Electromagnetic Research*, vol. 55, pp. 25-33, 2014.
[13] S. Sarkar, A. Majumdar, S. Mondal, S. Biswas, D. Sarkar and P. Sarkar, "Miniaturization of rectangular microstrip patch antenna using an optimized single-slotted ground plane", *Microwave and Optical Technology Letters*, vol. 53, pp. 111-115, 2011.
[14] S. Neogi, A. Bhattacharjee and P. Sarkar, "Size reduction of rectangular microstrip antenna', *Microwave and Optical Technology Letters*, vol. 56, pp. 244-248, 2014.
[15] T. Chiou and K. Wong, "Designs of Compact Microstrip Antennas with a Slotted ground plane", *IEEE Antennas and Propagation Society International Symposium*, vol. 2, pp. 732-735, 2001.
[16] U. Chakraborty, S. K. Chowdhury and A. K. Bhattacharjee, "Frequency tuning and miniaturization of square microstrip antenna embedded with 't' shape defected ground structure", *Microwave and Optical Technology Letters*, vol. 55, pp. 869-872, 2013.
[17] K. Mondal and P. Sarkar, "High gain wide-band U-shape patch antennas with modified ground planes", *IEEE transactions of Antennas and Propagation*, vol. 61, pp. 2279-2282, 2013.

received 4 Oct 2021; for review 5 Nov 2021; accepted 28 Mar 2022

ISSN 2179-1074

[18] S. Baudha and M. V. Yadav, "A novel design of a planar antenna with modified patch and defective ground plane for ultra-wideband applications", *Microwave and Optical Technology Letters*, vol. 61, pp. 1320-1327, 2019.
[19] A. U. Pawar, S. Chakraborty, L. L. Singh and S. Chattopadhyay, "Application of defected ground structure for augmenting high gain ultra-wide bandwidth from rectangular microstrip antenna", *Electromagnetics*, vol. 38, pp. 123-133, 2018.
[20] U. Chakraborty, S. Chowdhury and A. Bhattacharjee, "Compact dual-band microstrip antenna for IEEE 802.11a WLAN Application", *Antenna and Wave Propagation Letter*, vol. 13, pp. 407-410, 2014.
[21] T. Wang, Y. Z. Yin, J. Yang, Y. L. Zang and J. J. Xie, "Compact triple-band antenna using defected ground structure for WLAN/WiMAX applications", *Progress In Electromagnetic Research Letters*, vol. 35, pp. 155-164, 2012.
[22] N. Kishore, A. Prakash and V. S. Tripathi, "A multiband microstrip patch antenna with defected ground structure for its applications", *Microwave and optical technology letters*, vol. 58, pp. 2814-2818, 2016.
[23] A. Kunwar, A. Kumar and B. Kanaujia, "Inverted L-slot triple-band antenna with defected ground structure for WLAN and WiMAX applications", *International Journal of Microwave and Wireless Technologies*, vol. 9, pp. 1-6, 2015.
[24] T. Ali and R. Biradar, "A triple-band highly miniaturized antenna for WiMAX/WLAN applications", *Microwave and Optical Technology Letters*, vol. 60, pp. 466-471, 2018.
[25] C. Kumar and D. Guha, "Reduction in Cross-Polarized Radiation of Microstrip Patches using Geometry Independent resonant-type defected ground structure", *IEEE transactions of Antennas and Propagation*, vol. 63, pp. 2767-2772, 2015.
[26] C. Kumar and D. Guha, "Asymmetric geometry of defected ground structure for rectangular microstrip: A new approach to reduce its cross-polarized fields", *IEEE transactions of Antennas and Propagation*, vol. 64, pp. 2503-2506, 2016.
[27] A. Ghosh, S. Chakraborty, S. Chattopadhyay, A. Nandi and B. Basu, "Rectangular microstrip antenna with dumbbell shape defected ground structure for improved cross-polarized radiation in wide elevation angle and its theoretical analysis", *IET Microwaves, Antennas & Propagation*, vol. 10, pp. 68-78, 2016.
[28] C. Kumar and D. Guha, "Asymmetric and compact DGS configuration for circular patch with improved radiations", *IEEE Antennas and Wireless Propagation Letters*, vol. 19, pp. 355-357, 2020.
[29] D. Dutta, S. K. Rafidul, D. Guha, and C. Kumar, "Suppression of cross-polarized fields of microstrip patch across all skewed and orthogonal radiation Planes", *IEEE Antenna and Wireless propagation letters*, vol. 19, pp. 99-103, 2020.
[30] C. Sarkar, D. Guha, C. Kumar and Y. M. Antar, "New insight and design strategy to optimize cross-polarized radiations of Microstrip patch over full bandwidth by probe current control", *IEEE Transactions of Antennas and Propagation*, vol. 66, pp. 3902-3909, 2018.
[31] R. Garg, P. Bhartia, I. Bahl and A. Ittipiboon, Microstrip Antenna Design Handbook, Artech House, USA, 2001.
[32] CST, Microwave Studio 2019.
[33] P. A. Kadam and A. A. Deshmukh, "Designs of Regular Shape Microstrip Antennas Backed by Bow-tie Shape Ground Plane for Enhanced Antenna Characteristics", *AEU International Journal of Electronics and Communication*, vol. 137, pp. 1-9, 2021.
[34] D. Guha and Y. M. M. Antar, Microstrip and Printed Antennas New Trends, Techniques and Applications, Wiley and Sons publication, 2011.

received 4 Oct 2021; for review 5 Nov 2021; accepted 28 Mar 2022

ISSN 2179-1074